Original Article
Yonsei Med J 2020 Aug;61(8):679-688
https://doi.org/10.3349/ymj.2020.61.8.679
Yonsei Medical Journal
YMJ
pISSN: 0513-5796 · eISSN: 1976-2437

Cell Division Cycle 2 Protects Neonatal Rats Against Hyperoxia-Induced Bronchopulmonary Dysplasia

Zhongying Li[1], Yanhong Chen[2], Wenrong Li[3], and Fan Yan[4]

Departments of [1]Pediatric, [2]Pediatric Intensive Care, and [3]Pediatric Neurology and Rehabilitation, Binzhou People's Hospital, Binzhou; [4]Department of Pediatric II, The First Hospital of Yulin City, Yulin, China.

Purpose: Hyperoxia-induced bronchopulmonary dysplasia (BPD) is a lung disease in preterm infants. We aimed to explore the role of cell division cycle 2 (CDC2) on histopathologic changes of lung tissues, as well as the viability, apoptosis, and inflammation of lung cells in rats with hyperoxia-induced BPD.

Materials and Methods: Hyperoxia-induced BPD in neonatal rats and hyperoxia-induced A549 cells were constructed. The mRNA expression of CDC2 was detected by qRT-PCR. The fibrosis score of lung tissues was evaluated by hematoxylin-eosin staining. The viability and apoptosis of A549 cells were detected by cell counting kit-8 assay and flow cytometry. The protein expressions of bcl-2, bax, and caspase-3 were measured by western blot. The levels of tumor necrosis factor-α (TNF-α), interleukin (IL)-6, and IL-1β in A549 cells were detected by enzyme-linked immunosorbent assay. The pcDNA3.1-CDC2 was injected into rats to determine the role of CDC2 in hyperoxia-induced BPD in vivo.

Results: The expression of CDC2 was decreased in lung tissues of neonatal rats with hyperoxia-induced BPD and hyperoxia-induced A549 cells. The fibrosis score was increased in the lung tissues of neonatal rats with hyperoxia-induced BPD. Overexpression of CDC2 increased the viability and protein expression of bcl-2; and inhibited the apoptosis, inflammation, and protein expression of bax and caspase-3 in hyperoxia-induced A549 cells. Up-regulation of CDC2 alleviated the histopathologic changes in lung tissues of neonatal rats with hyperoxia-induced BPD.

Conclusion: Overexpression of CDC2 promoted the viability and inhibited the apoptosis and inflammation of hyperoxia-induced cells, and alleviated the histopathologic changes of lung tissues in neonatal rats with hyperoxia-induced BPD.

Key Words: CDC2, hyperoxia-induced bronchopulmonary dysplasia, viability, apoptosis, inflammation

INTRODUCTION

Bronchopulmonary dysplasia (BPD) is a lung disease commonly found in preterm infants.[1] The pathophysiology of BPD is characterized by poor alveolarization, disrupted microvascular development, mesenchymal cell hyperplasia, and fibrosis.[2] The incidence of BPD is 68% among preterm infants at 22–28 weeks of gestation.[3] BPD is most closely related to preterm birth; and other factors, such as prenatal infection and inflammation, mechanical ventilation, oxygen toxicity with decreased host antioxidant defenses, patent ductus arteriosus, and postnatal infection, all contribute to the pathogenesis of BPD.[4] Northway, et al.[5] proposed the following four major factors in the pathogenesis of BPD: lung immaturity, respiratory failure, oxygen supplementation, and positive-pressure mechanical ventilation. Beyond these factors, new knowledge suggests additional complex processes involved in the pathogenesis of BPD, including inflammation, aberrations in lung growth and lung signaling pathways, as well as derangements in transcription factors and growth factors.[6] The pathogenesis of BPD is complex, and there is yet no effective and safe therapy for this condition. Therefore, it is essential to explore new approaches for the treatment of BPD.

Hyperoxia is a leading cause of BPD, which can enhance cell

Received: February 19, 2020 **Revised:** June 5, 2020
Accepted: June 25, 2020
Corresponding author: Fan Yan, MM, Department of Pediatric II, The First Hospital of Yulin City, No. 59, Wenhua Road, Suide County, Shaanxi Province 718000, China. Tel: 86-0912-5641782, Fax: 86-0912-5641782, E-mail: yanfan1680@163.com

•The authors have no potential conflicts of interest to disclose.

injury in alveolar epithelial and endothelial cells.[7] Preterm infants are more susceptible to hyperoxia-induced BPD due to perinatal infection and inflammation,[8] respiratory immaturity,[9] and oxidative stress.[10] Hyperoxia exposure in neonatal rats causes alveolar development deficits and inflammation similar to pathological features in preterm infants with BPD.[11] Currently, hyperoxia-induced BPD is mainly treated by corticosteroids and mechanical ventilation.[12,13] However, their modest effectiveness is accompanied by severe side effects on alveolar growth and neural development. The treatment of preterm infants with hyperoxia-induced BPD should be further explored.

Lung development requires an ordered pattern of proliferation and differentiation of various lung cells that culminates in the development of alveolus, airways, and various specialized cells that are required for air breathing.[14] Therefore, normal cell-cycle progression is crucial for lung development. The cell division cycle 2 (CDC2), which belongs to CDC genes, is involved in the cell cycle.[15] In a normal cell cycle, the activation of CDC2 is a key event in triggering the transition from G2 phase to mitotic phase, by promoting the breakdown of the nuclear membrane, chromatin condensation, and microtubule spindle formation.[16] In the past, the relationship between CDC genes and lung diseases mainly focused on cancers. CDC2 has been observed in early stage lung adenocarcinomas.[17] Overexpression of CDC20 is related to poor prognosis in the lung adenocarcinoma,[18] and is found in the Fine Particulate Matter ($PM_{2.5}$)-induced lung cancers cells.[19] Up-regulation of CDC-associated 3 protein inhibits the tumorigenesis of non-small-cell lung cancer.[20] However, the role of CDC2 in preterm infants with hyperoxia-induced BPD is unknown.

In this study, we evaluated the histopathologic changes of lung tissues in neonatal rats with hyperoxia-induced BPD. Then, we explored the regulatory effects of CDC2 on the viability, apoptosis, and inflammation of hyperoxia-induced A549 cells. Finally, the role of CDC2 was determined in neonatal rats with hyperoxia-induced BPD. The results of this study may provide a new approach for the treatment of hyperoxia-induced BPD in preterm infants.

MATERIALS AND METHODS

Animals

Sixty neonatal Wistar rats (4.0±0.43 g) were purchased from the Institute of Zoology, Chinese Academy of Sciences (Beijing, China). The rats were fed standard chow and water, while being maintained under a 12 h/12 h light/dark cycle. This study was approved by the Animal Ethics Committee (No: 190) of our hospital, and all experiments were conducted in accordance with the NIH Guide for the Care and Use of Laboratory. After the study, all animals were anesthetized by intraperitoneal injection of sodium pentobarbital (80 mg/kg), and then sacrificed by cervical dislocation.

Hyperoxia-induced BPD model

Hyperoxia-induced BPD model in neonatal rats (2–3 days old) was established by exposing in an atmosphere of 90% oxygen (O_2) and <5% carbondioxide (CO_2) with continuous O_2 monitoring for 7 days. The neonatal rats with hyperoxia-induced BPD were divided into Model, Model+pcDNA, and Model+pcDNA-CDC2 groups (15 rats in each group). The neonatal rats with hyperoxia-induced BPD were intravenously injected with 100 μg of pcDNA (Model+pcDNA group) or pcDNA-CDC2 (Model+pcDNA group) in a large volume of saline (2 mL), in accordance with the method previously reported by Lewis and Wolff[21] at 7, 10, and 13 days after hyperoxia induction. The rats (n=15) in the control group were kept in room air (normoxia, 21% oxygen) without treatment. At 3, 7, and 14 days after hyperoxia induction, the rats were anesthetized with 50 mg/kg pentobarbital sodium, and sacrificed by cervical dislocation. The three groups of rats received 0, 1, and 3 times of pcDNA or pcDNA-CDC2 injection, respectively. Lung tissues were collected for future experiments.

Histopathology of lung tissues

Lung tissues were fixed in 4% paraformaldehyde for 24 h, embedded in paraffin, cut into sections at 6-μm thickness, and underwent hematoxylin-eosin (HE) staining. By means of light microscopy (Nikon, Eclipse 80i, Tokyo, Japan), the expansion of the alveoli and pulmonary interstitial of lung tissues were observed. The fibrosis score was graded as previously described.[22] In brief, the extent of pathological lesions was graded from 0 to 3, as shown in Table 1. A perpendicular line was drawn from the center of the most peripheral bronchiole to the nearest interlobular septum, and the alveoli were counted along the line, which reflects the degree of alveolarization and the extent of lung development/injury. At least three sections were evaluated for each mouse, counting was done five times for each section, and a mean was obtained as the radial alveolar count (RAC) Image-Pro Plus 6.0 software (IPP, Media Cybernetics, Rockville, MD, USA) was used to detect the mean alveolar diameter (MAD) and alveolar septal thickness (AST). The mean linear chord length (Lm), as an indication of MAD, was calculated by dividing the length of seven horizontal test lines placed 40 mm apart (total length=2968 mm) by the number of intercepts of the septal wall. The same measurements were done over at least four different areas of the lung section (superior and inferior sections of each lung). AST was determined near the center of septae from 30 to 40 different alveoli in each section, as described recently in lungs of mice.[23] At least three different sections from each lung were used for these measurements.

Cell culture

A549 cells (human respiratory epithelium) were obtained from American Type Culture Collection (ATCC, Manassas, VA, USA). All cell lines were cultured in Roswell Park Memorial Institute (RPMI)-1640 (GIBCO, Erie, NY, USA) with 10% fetal

https://doi.org/10.3349/ymj.2020.61.8.679

Table 1. Quantitative Histopathology Score of Lung Injury

Tissue	0	1	2	3
Alveolar septae	All septae are thin and delicate	Congested alveolar septae in less than 1/3 of the field	Congested alveolar septae in 1/3 to 2/3 of the field	Congested alveolar septae in greater than 2/3 of the field
Alveolar hemorrhage	No hemorrhage	At least 5 erythrocytes per alveolus in 1 to 5 alveoli	At least 5 erythrocytes per alveolus in 5 to 10 alveoli	At least 5 erythrocytes per alveolus in more than 10 alveoli
Intra-alveolar fibrin	No intra-alveolar fibrin	Fibrin strands in less than 1/3 of the field	Fibrin strands in 1/3 to 2/3 of the field	Fibrin strands in greater than 2/3 of the field
Intra-alveolar infiltrates	Less than 5 intraalveolar cells per field	5 to 10 intra-alveolar cells per field	10 to 20 intraalveolar cells per field	More than 20 intraalveolar cells per field

bovine serum (FBS, Invitrogen, Carlsbad, CA, USA) at 37°C containing 5% CO_2. Hyperoxia was used to construct the BPD model in A549 cells (A549 cells were conducted in a humidified chamber flushed with 95% O_2, 5% CO_2 at 37°C for 6 h). The Air group cells were cultured constantly under normal conditions in a normal medium.

Cell transfection

The pcDNA3.1-CDC2 and pcDNA3.1-negative control (NC) were obtained from Shanghai Genepharma (Shanghai, China). The hyperoxia-induced A549 cells were grown to 60% confluence, and then harvested for the experiment. The cells were divided into the following three groups: Hyperoxia group (hyperoxia-induced A549 cells without transfection); Hyperoxia+pcDNA-NC group (hyperoxia-induced A549 cells were transfected with pcDNA3.1-NC); Hyperoxia+pcDNA-CDC2 group (hyperoxia-induced A549 cells were transfected with pcDNA3.1-CDC2). Transfections were performed using Lipofectamine 3000 reagent (Invitrogen).

Cell viability assay

To measure the cell viability, hyperoxia-induced A549 cells were seeded in 96-well plates. Then, 10 μL of cell counting kit-8 (CCK-8) reagents (BD Biosciences, Franklin Lakes, NJ, USA) were separately added into each well of the 96-well plate. The optical density 450 nm (OD_{450}) was measured using a microplate reader (BioTek Instruments Inc., Winooski Vermont, WV, USA). Lactate dehydrogenase (LDH) released in the cell culture media was monitored by using the LDH activity kit (Nanjing Jiancheng Bioengineering Institute, Nanjing, China). LDH release is presented as % cytotoxicity.

Flow cytometry

Apoptosis was detected using the Annexin V-PI kit (Invitrogen). A549 cells were seeded in 96-well plates, and cultured for 24 h. Then cells were stained with 5 μL Annexin V-fluorescein isothiocyanate and 10 μL propidium iodide for 15 min in the dark. The apoptosis rate was detected on flow cytometry (BD Biosciences).

Enzyme-linked immunosorbent assay

The supernatant of transfected cells was collected, and the levels of the tumor necrosis factor-α (TNF-α), interleukin (IL)-1β, and IL-6 were measured by enzyme-linked immunosorbent assay (ELISA) kits (R&D systems, Inc., Mineapolis, MN, USA). Absorbance was measured at 450/550 nm by enzyme mark instrument (Molecular Devices, Sunnyvale, CA, USA).

Quantitative real-time polymerase chain reaction

Total RNA was extracted from lung tissues or cells using the TRIzol reagent (Invitrogen), and was reverse-transcribed into cDNA by Takara PrimeScript RT reagent kit (Takara, Otsu, Japan). PCR reaction was performed on ABI 7500HT Fast Real-Time PCR System (Applied Biosystems, Waltham, MA, USA) under the following conditions: 95°C for 3 min, 40 cycles of 95°C for 15 s, and 60°C for 30 s. Relative expression was calculated by the $2^{-\Delta\Delta Ct}$ method. β-actin was used for the normalization. The primer sequences are shown in Supplementary Table 1 (only online).

Western blot

Lung tissues and A549 cells were lysed by ice-cold lysis buffer to obtain the total protein. The concentration of total protein was detected by bicinchoninic acid protein concentration assay kit (Pierce, Rockford, IL, USA). Protein samples were separated in sodium dodecyl sulfate polyacrylamide gel electrophoresis, and transferred onto polyvinylidene fluoride membrane. Then, the membranes were incubated with primary antibody overnight at 4°C. The antibodies used in this study were as follows: anti-cyclin-dependent kinases (1:1000, ab131450, Abcam, Cambridge, MA, USA), anti-Bcl-2 (1:1000, ab182858, Abcam), anti-Bax-2 (1:1000, ab32503, Abcam), and anti-Cleaved Caspase-3 (1:1000, ab2302, Abcam). The membranes were then incubated with horseradish peroxidase-labeled goat anti-rabbit IgG (1:5000, ab6712, Abcam) secondary antibody for 1 h at room temperature. Finally, the protein bands were visualized by enhanced chemiluminescence exposure solution, and quantified by a gel imaging system (UVP, Upland, CA, USA). GAPDH (1:1000, ab181602, Abcam) was introduced as the internal reference.

Statistical analysis

Statistical analysis was performed with SPSS 23.0 (IBM, Corp., Armonk, NY, USA). Data are presented as mean±standard de-

viation. The differences among various groups were analyzed by one-way ANOVA, followed by Tukey's multiple comparisons test. p value<0.05 was considered statistically significant.

RESULTS

Hyperoxia-induced BPD enhanced histopathologic changes in lung tissues of neonatal rats

The expansion of the alveoli, pulmonary interstitial fibrosis, and fibrosis score of lung tissues were evaluated by HE staining. By contrast to the control group, expansion of the alveoli and pulmonary interstitial fibrosis were more obvious in the model group (Fig. 1A). The fibrosis score in the model group was higher than that in the control group on days 7 and 14 (p<0.001) (Fig. 1B). The alveolar area and RAC value were markedly decreased in the model group on days 7 and 14 compared to the control group (p<0.01) (Fig. 1C and D). The MAD and AST were in contrast with the RAC value (p<0.01) (Fig. 1E and F).

CDC2 expression was decreased in neonatal rats with hyperoxia-induced BPD

The relative mRNA expression of CDC2 was detected by qRT-PCR. Compared to the control group, the relative mRNA expression of CDC2 in lung tissues was markedly decreased in the model group on days 7 and 14 (p<0.01) (Fig. 2A). The relative protein expression of CDC2 was detected by western blot. By contrast to the control group, the relative protein of CDC2 in lung tissues was markedly decreased in the model group on days 7 and 14 (p<0.01) (Fig. 2B).

CDC2 enhanced viability and reduced apoptosis of hyperoxia-induced A549 cells

We then investigated the effect of CDC2 on hyperoxia-induced BPD in vitro. We performed hyperoxia induction to produce hyperoxia-induced BPD in A549 cells. According to qRT-PCR and western blot analysis, the relative mRNA and protein expression of CDC2 was down-regulated in hyperoxia-induced A549 cells (p<0.01) (Fig. 3A and B). Transfection with pcDNA3.1-CDC2 markedly increased the expression of CDC2 protein in hyperoxia-induced A549 cells (p<0.001) (Fig. 3C). The biological effect of CDC2 on cell viability was assessed by CCK-8 assay. Cell viability was decreased in hyperoxia-induced A549 cells (p<0.001). Up-regulation of CDC2 markedly increased the cell viability in hyperoxia-induced A549 cells (p<0.001) (Fig. 3D and E). Flow cytometry assay was utilized to analyze the apoptosis rate of A549 cells. The cell apoptosis rate in the Hyperoxia group was higher than that in the Air group (p<0.001). In contrast to the Hyperoxia group, the cell apoptosis rate was markedly decreased in the Hyperoxia+pcDNA-CDC2 group (p<0.001) (Fig. 3F). Meanwhile, the relative protein expressions of bcl-2, bax, and caspase-3 were detected by western blot. Compared with the Air group, hyperoxia exposure markedly down-regulated the relative protein expression of bcl-2, and up-regulated bax and caspase-3 in A549 cells (all p<0.001). Transfection with pcDNA3.1-CDC2 markedly increased the relative protein expression of bcl-2, and decreased bax and caspase-3 in hyperoxia-induced A549 cells (all p<0.001) (Fig. 3G).

Effect of CDC2 on the cell cycle phases of hyperoxia-induced A549 cells

The proportion of G0/G1, S, and G2/M phase cells were detected by flow cytometry. Our results revealed that the number

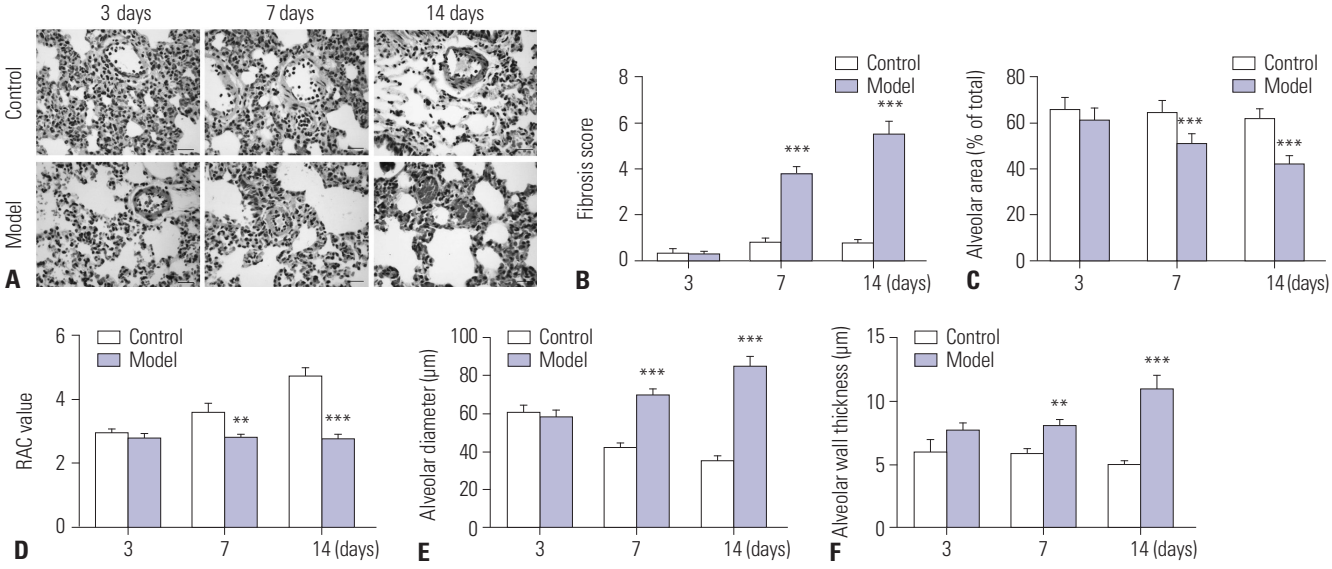

Fig. 1. Hyperoxia-induced bronchopulmonary dysplasia enhanced histopathologic changes of lung tissues in neonatal rats. (A and B) The expansion of the alveoli, pulmonary interstitial fibrosis, and fibrosis score of lung tissues were evaluated by hematoxylin-eosin staining. (C) Alveolar area. (D) RAC value. (E) Mean alveolar diameter. (F) Alveolar septal thickness. Control, neonatal rats were kept in room air; Model, neonatal rats were exposed to an atmosphere of 90% oxygen (O_2) and <5% carbondioxide (CO_2). **p<0.01, ***p<0.001 vs. Control. RAC, radical alveolar counts.

https://doi.org/10.3349/ymj.2020.61.8.679

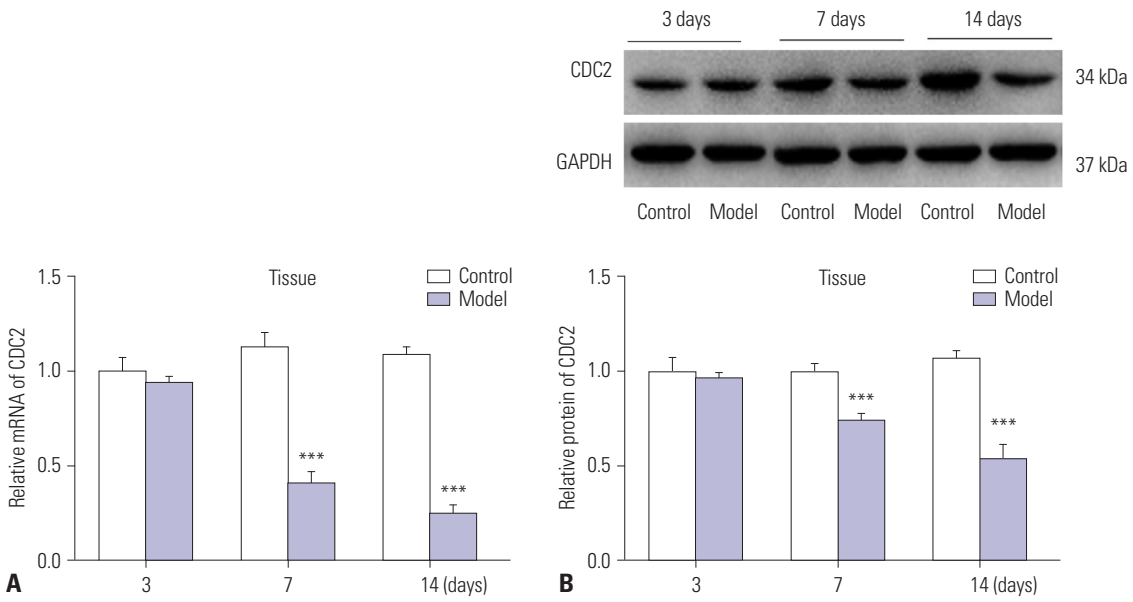

Fig. 2. The CDC2 expression was decreased in neonatal rats with hyperoxia-induced bronchopulmonary dysplasia. (A) The relative mRNA expression of CDC2 was detected by qRT-PCR. (B) The relative protein expression of CDC2 was detected by western blot. Control, neonatal rats were kept in room air; Model, neonatal rats were exposed to an atmosphere of 90% oxygen (O_2) and <5% carbondioxide. ***p<0.001 vs. Control. CDC, cell division cycle 2.

of cells was markedly decreased in the G0/G1 phases, and increased in the S and G2/M phases in the Hyperoxia group compared to the Air group (all p<0.001). Treatment with pcDNA3.1-CDC2 significantly elevated the number of cells in the G0/G1 phases (p<0.01), and reduced the number of cells in the S and G2/M phases in hyperoxia-induced A549 cells (p<0.05) (Fig. 4).

CDC2 decreased the secretion of proinflammatory cytokines in hyperoxia-induced A549 cells

To evaluate the effect of CDC2 on inflammation of hyperoxia-induced A549 cells, we examined the levels and the relative mRNA expression of TNF-α, IL-1β, and IL-6 in A549 cells using ELISA and qRT-PCR. The results displayed that the levels of TNF-α, IL-1β, and IL-6 in A549 cells in the Hyperoxia group were higher than that in the Air group (p<0.001). Overexpression of CDC2 markedly decreased the above indexes in hyperoxia-induced A549 cells (p<0.01) (Fig. 5A-C). qRT-PCR showed that the relative mRNA expressions of TNF-α, IL-1β, and IL-6 in A549 cells in the Hyperoxia group were higher than those in the Air group (p<0.001). Up-regulation of CDC2 markedly inhibited the relative mRNA expressions of TNF-α, IL-1β, and IL-6 in hyperoxia-induced A549 cells (p<0.01) (Fig. 5D-F).

CDC2 alleviated the histopathologic changes of lung tissues in neonatal rats with hyperoxia-induced BPD

According to qRT-PCR, the relative mRNA expression of CDC2 was increased in the Model+pcDNA-CDC2 group compared to the Model group (p<0.001) (Fig. 6A). HE staining showed that the expansion of the alveoli and pulmonary interstitial fibrosis were less obvious in the Model+pcDNA-CDC2 group compared to the Model group (Fig. 6B). Up-regulation of CDC2 markedly decreased the fibrosis score in lung tissues of neonatal rats with hyperoxia-induced BPD (p<0.001) (Fig. 6C). Compared with the Model group, the alveolar area and RAC value were markedly increased in the Model+pcDNA-CDC2 group (p<0.001) (Fig. 6D and E). The results of IPP analysis revealed that injection with pcDNA3.1-CDC2 markedly decreased the MAD and AST of neonatal rats with hyperoxia-induced BPD (p<0.001) (Fig. 6F and G).

DISCUSSION

Hyperoxia may cause BPD in immature lungs of preterm infants.[24] The hyperoxia-induced BPD model in neonatal rat is commonly recognized as a suitable model of BDP in preterm infants.[25] In order to explore an appropriate therapy for BPD, we constructed a hyperoxia-induced BPD model in rats. In this study, the expansion of the alveoli and pulmonary interstitial fibrosis were obvious; RAC value was decreased; and the fibrosis score, MAD, and AST were increased at 7 and 14 days after hyperoxia induction. All of these factors suggest that the hyperoxia-induced BPD rat model was constructed successfully.

An abnormal expression of CDC gene is related to the progress of pediatric disease. For instance, the expression of hCDCrel (human cell division cycle related) was decreased in infants with acute myeloid leukemia.[26] CDC42 was down-regulated in the pediatric inflammatory bowel disease.[27] In this study, the protein and mRNA expressions of CDC2 in lung tissues were markedly decreased in the Model group on days 7 and 14 and

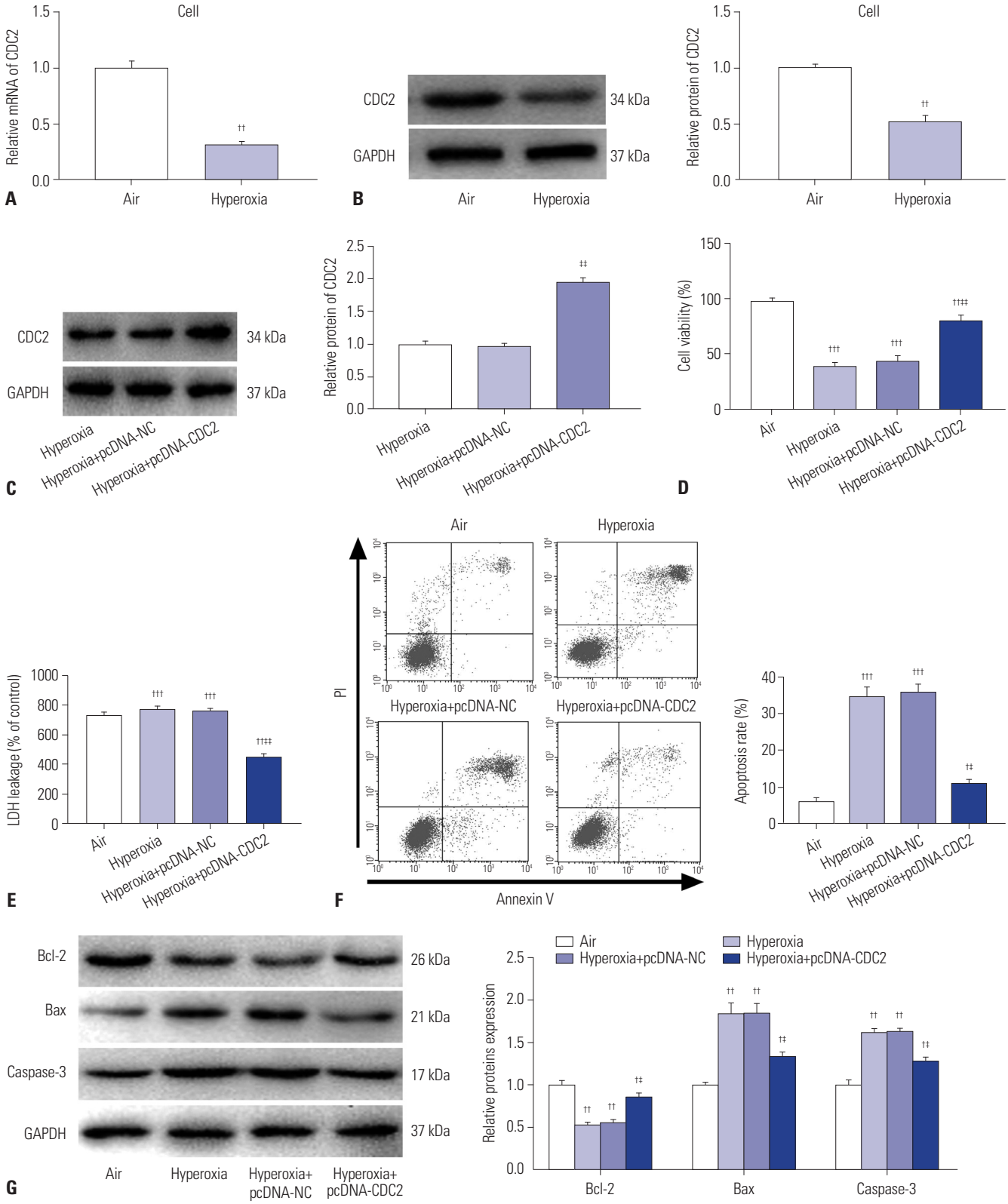

Fig. 3. CDC2 enhanced the viability and reduced the apoptosis of hyperoxia-induced A549 cells. (A) The relative mRNA expression of CDC2 was detected by qRT-PCR. (B) The protein bands of CDC2 in A549 cells. (C) The relative protein expression of CDC2 was detected by western blot. (D) Cell viability was assessed by cell counting kit-8 assay. (E) Cell viability was assessed by LDH assay. (F) Cell apoptosis rate was detected by flow cytometry. (G) The relative protein expressions of bcl-2, bax, and caspase-3 were measured by western blot. Air, A549 cells were kept in room air; Hyperoxia, A549 cells were exposed to an atmosphere of 90% oxygen (O_2) and <5% carbondioxide (CO_2); Hyperoxia+pcDNA-NC, hyperoxia-induced A549 cells were transfected with pcDNA-NC; Hyperoxia+pcDNA-CDC2, hyperoxia-induced A549 cells were transfected with pcDNA-CDC2. $^{\dagger}p<0.05$, $^{\dagger\dagger}p<0.01$, $^{\dagger\dagger\dagger}p<0.001$ vs. Air; $^{\ddagger}p<0.05$, $^{\ddagger\ddagger}p<0.01$ vs. Hyperoxia and Hyperoxia+pcDNA-NC. CDC, cell division cycle 2; LDH, lactate dehydrogenase.

https://doi.org/10.3349/ymj.2020.61.8.679

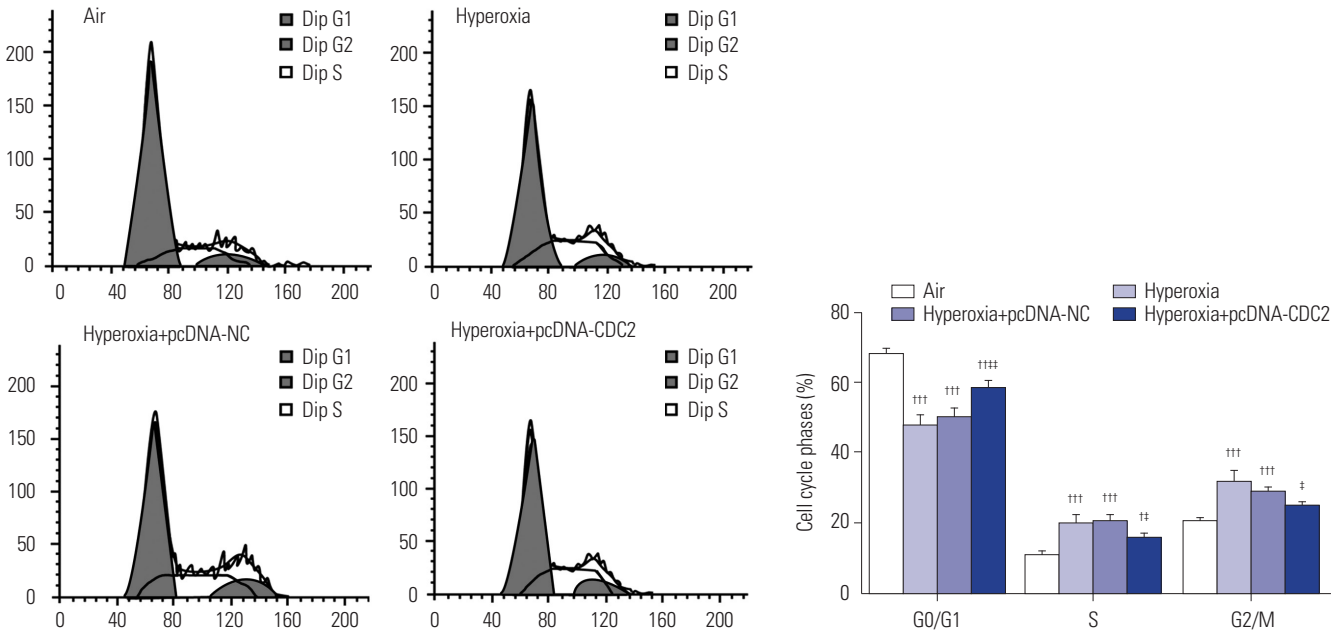

Fig. 4. Effect of CDC2 on the cell cycle phases of hyperoxia-induced A549 cells. The cell cycle phases of G0/G1, S, and G2/M. Air, A549 cells were kept in room air; Hyperoxia, A549 cells were exposed to an atmosphere of 90% oxygen (O_2) and <5% carbondioxide (CO_2); Hyperoxia+pcDNA-NC, hyperoxia-induced A549 cells were transfected with pcDNA-NC; Hyperoxia+pcDNA-CDC2, hyperoxia-induced A549 cells were transfected with pcDNA-CDC2. $^{\dagger}p<0.05$, $^{\dagger\dagger}p<0.01$, $^{\dagger\dagger\dagger}p<0.001$ vs. Air; $^{\ddagger}p<0.05$, $^{\ddagger\ddagger}p<0.01$ vs. Hyperoxia and Hyperoxia+pcDNA-NC. CDC, cell division cycle 2.

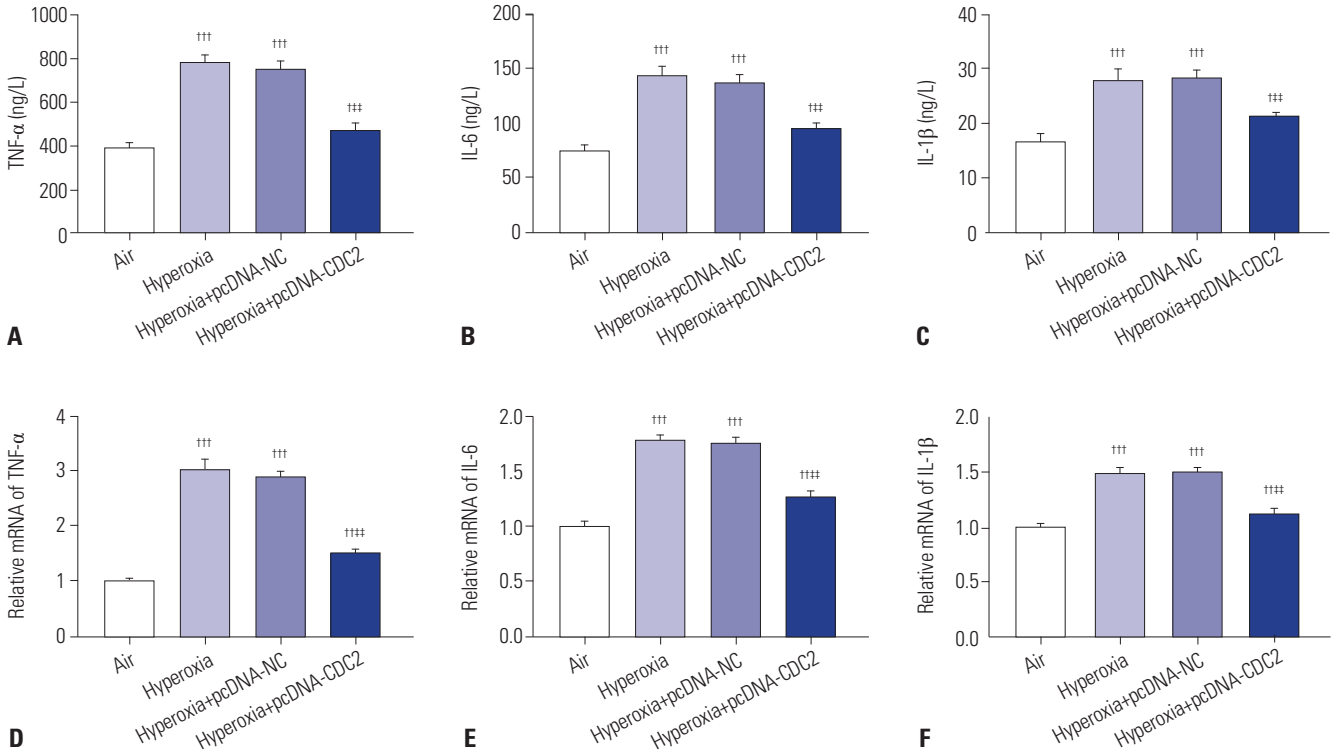

Fig. 5. CDC2 decreased the secretion of proinflammatory cytokines in hyperoxia-induced A549 cells. (A-C) The levels of tumor necrosis factor-α (TNF-α), interleukin (IL)-6, and IL-1β in A549 cells were measured by enzyme-linked immunosorbent assay. (D-F) The relative mRNA expression of TNF-α, IL-6, and IL-1β in A549 cells was measured by qRT-PCR. Air, A549 cells were kept in room air; Hyperoxia, A549 cells were exposed to an atmosphere of 90% oxygen (O_2) and <5% carbondioxide (CO_2); Hyperoxia+pcDNA-NC, hyperoxia-induced A549 cells were transfected with pcDNA-NC; Hyperoxia+pcDNA-CDC2, hyperoxia-induced A549 cells were transfected with pcDNA-CDC2. $^{\dagger}p<0.05$, $^{\dagger\dagger}p<0.01$, $^{\dagger\dagger\dagger}p<0.001$ vs. Air; $^{\ddagger\ddagger}p<0.01$ vs. Hyperoxia and Hyperoxia+pcDNA-NC. CDC, cell division cycle 2.

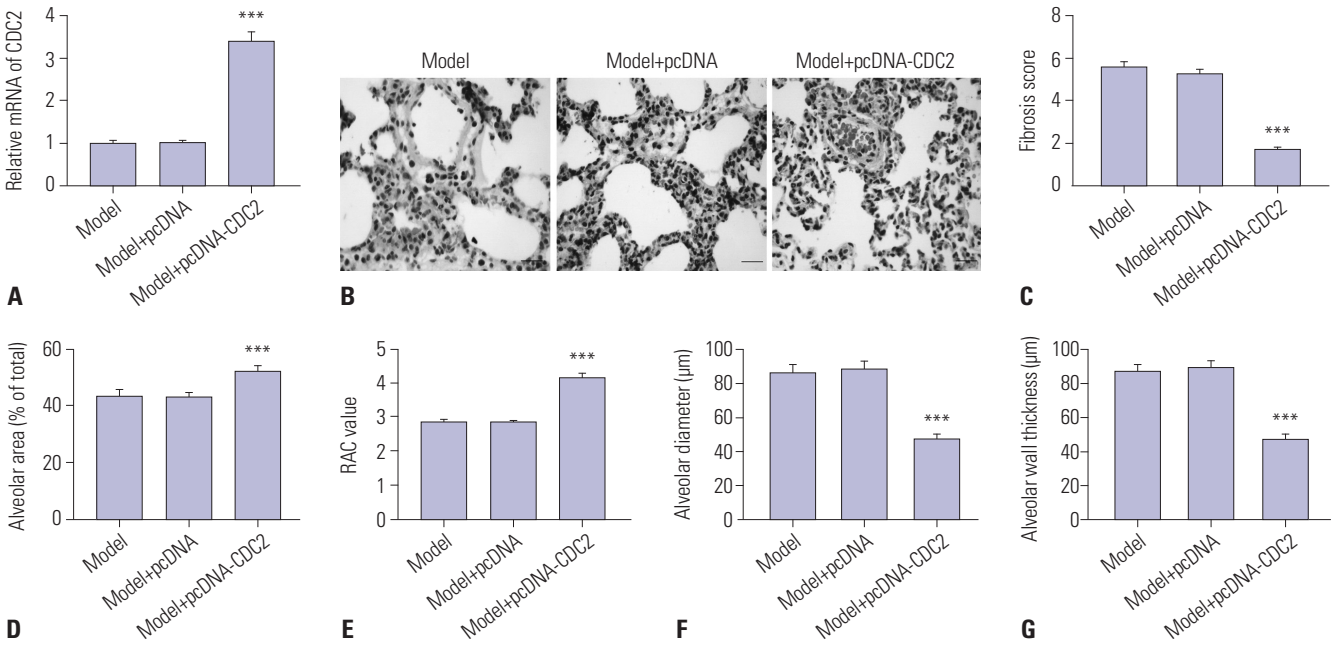

Fig. 6. CDC2 alleviated the histopathologic changes of lung tissues in neonatal rats with hyperoxia-induced bronchopulmonary dysplasia (BPD). (A) The relative mRNA expression of CDC2 in lung tissues was measured by qRT-PCR. (B and C) The expansion of the alveoli, pulmonary interstitial fibrosis, and fibrosis score of lung tissues were evaluated by hematoxylin-eosin staining. (D) The alveolar area. (E) Radical alveolar counts (RAC) value. (F and G) Mean alveolar diameter and alveolar septal thickness were measured by Image-Pro Plus 6.0 software. Model, neonatal rats were exposed to an atmosphere of 90% oxygen (O_2) and <5% carbondioxide (CO_2); Model+pcDNA, neonatal rats with hyperoxia-induced BPD were injected with pcDNA; Model+pcDNA-CDC2, neonatal rats with hyperoxia-induced BPD were injected with pcDNA-CDC2. ***p<0.001 vs. Model and Model+pcDNA. CDC, cell division cycle 2.

in hyperoxia-induced A549 cells. The results suggest that CDC2 may play important roles in regulating hyperoxia-induced BPD. Numerous studies have indicated that the cell viability and apoptosis play critical roles in the occurrence and development process of BPD in preterm infants.[28] Long non-coding RNA MALAT1 alleviates the BPD in preterm infants by promoting cell proliferation and inhibiting cell apoptosis.[29] Supplementation of glutamine protects against BPD by increasing the cell viability and decreasing the cell apoptosis of hyperoxia-induced A549 cells.[30] In this study, up-regulation of CDC2 enhanced the cell viability and attenuated the cell apoptosis of hyperoxia-induced A549 cells. Up-regulation of CDC2 also decreased the protein expression of bcl-2, and increased bax and caspase-3 in hyperoxia-induced A549 cells, implying a functional interaction between CDC2 and cell apoptosis.

CDC gene plays a key role in regulating the cell cycle. Hansel, et al.[31] has found that the CDC2 not only regulates G1 progress and G1/S transition, but also is capable of promoting G2/M transition through an association with multiple interphase cyclins. Cyclin B1 combines with CDC2 to form a complex. Once activated, this complex can initiate cells to progress from the G1/S phase to the G2/M phase.[32] A previous study has reported that drugs can act on and inhibit the cyclin B1/CDC2 complex, which delays the G2/M phase and inhibits cell growth.[33] In the present study, overexpression of CDC2 increased the number of hyperoxia-induced A549 cells in the G0/G1 phases, and reduced the number in the S and G2/M phase. Hyperoxia prevents lung development by inhibiting proliferation in the G1 phase and increasing arresting in the S phase.[34] We suspect that CDC2 may protect A549 cells against hyperoxia-induced BPD by mediating the G0/G1, S, and G2/M phases.

Inflammation plays a key role in the pathological mechanisms of preterm infants with BPD.[35] Previous evidence has shown that the inhibition of proinflammatory cytokines can ameliorate BPD.[36] Wu, et al.[37] also indicated that CDC2 is a positive regulator of the interferon (IFN) signaling pathway. The increased expression of CDC2 in systemic lupus erythematosus contributes to the over-activation of type I IFN signaling. Du, et al.[38] found that the inhibition of CDC2 significantly decreased lipopolysaccharide (LPS)-induced nitric oxide production, indicating that CDC2 mediates macrophage activation by LPS. In this study, overexpression of CDC2 decreased the levels and relative mRNA expression of proinflammatory cytokines in hyperoxia-induced A549 cells. Overexpression of CDC2 decreased the expansion of the alveoli, pulmonary interstitial fibrosis, fibrosis score, MAD, and AST; and increased the RAC value in neonatal rats with hyperoxia-induced BPD. Therefore, we speculated that high expression of CDC2 may relieve inflammation during the development of hyperoxia-induced BPD through inhibition of TNF-α, IL-6, and IL-1β-related signaling. Taken together, our results suggest that overexpression of CDC2 may serve as a potential target used in the treatment for hyperoxia-induced BPD in preterm infants.

https://doi.org/10.3349/ymj.2020.61.8.679

This study had a limitation. Since we focused on cell experiments in vitro, the cell viability, status apoptosis, and expression of inflammatory cytokines in lung tissues of experimental animals after exogenous DNA injection were not detected in the current study.

In summary, CDC2 was decreased in the lung tissues of neonatal rats with hyperoxia-induced BPD and hyperoxia-induced A549 cells. Overexpression of CDC2 increased the viability while decreasing the apoptosis and inflammation of hyperoxia-induced A549 cells. Up-regulation of CDC2 alleviated the histopathologic changes in lungs of rats with hyperoxia-induced BPD. CDC2 may act as a potential therapeutic target for hyperoxia-induced BPD in preterm infants. However, the detailed action mechanism of CDC2 on hyperoxia-induced BPD remains limited, and further research is still needed.

AUTHOR CONTRIBUTIONS

Conceptualization: Zhongying Li. Data curation: Zhongying Li and Yanhong Chen. Formal analysis: Zhongying Li and Yanhong Chen. Investigation: Zhongying Li and Wenrong Li. Methodology: Wenrong Li and Fan Yan. Project administration: all authors. Resources: Zhongying Li. Software: Fan Yan. Supervision: Zhongying Li. Validation: Zhongying Li , Yanhong Chen, and Fan Yan. Visualization: Zhongying Li. Writing—original draft: all authors. Writing—review & editing: Zhongying Li and Fan Yan. Approval of final manuscript: all authors.

ORCID iDs

Zhongying Li https://orcid.org/0000-0002-5130-3170
Yanhong Chen https://orcid.org/0000-0001-6506-0715
Wenrong Li https://orcid.org/0000-0003-1472-4491
Fan Yan https://orcid.org/0000-0001-5254-0488

REFERENCES

1. Baud O, Maury L, Lebail F, Ramful D, El Moussawi F, Nicaise C, et al. Effect of early low-dose hydrocortisone on survival without bronchopulmonary dysplasia in extremely preterm infants (PREMILOC): a double-blind, placebo-controlled, multicentre, randomised trial. Lancet 2016;387:1827-36.
2. Bach KP, Kuschel CA, Hooper SB, Bertram J, Mcknight S, Peachey SE, et al. High bias gas flows increase lung injury in the ventilated preterm lamb. PLoS One 2012;7:e47044.
3. Durrmeyer X, Kayem G, Sinico M, Dassieu G, Danan C, Decobert F. Perinatal risk factors for bronchopulmonary dysplasia in extremely low gestational age infants: a pregnancy disorder-based approach. J Pediatr 2012;160:578-83.e2.
4. Gien J, Kinsella JP. Pathogenesis and treatment of bronchopulmonary dysplasia. Curr Opin Pediatr 2011;23:305-13.
5. Northway WH Jr, Rosan RC, Porter DY. Pulmonary disease following respirator therapy of hyaline-membrane disease. Bronchopulmonary dysplasia. N Engl J Med 1967;276:357-68.
6. Lal CV, Ambalavanan N. Biomarkers, early diagnosis, and clinical predictors of bronchopulmonary dysplasia. Clin Perinatol 2015;42:739-54.
7. De Paepe ME, Mao Q, Chao Y, Powell JL, Rubin LP, Sharma S. Hyperoxia-induced apoptosis and Fas/FasL expression in lung epithelial cells. Am J Physiol Lung Cell Mol Physiol 2005;289:L647-59.
8. Kallapur GS, Jobe AH. Contribution of inflammation to lung injury and development. Arch Dis Child Fetal Neonatal Ed 2006;91:F132–5.
9. Fiaturi N, Russo JW, Nielsen HC, Castellot JJ Jr. CCN5 in alveolar epithelial proliferation and differentiation during neonatal lung oxygen injury. J Cell Commun Signal 2018;12:217-29.
10. Ratner V, Slinko S, Utkina-Sosunova I, Starkov A, Polin RA, Ten VS. Hypoxic stress exacerbates hyperoxia-induced lung injury in a neonatal mouse model of bronchopulmonary dysplasia. Neonatology 2009;95:299-305.
11. Zhu Y, Fu J, Yang H, Pan Y, Yao L, Xue X. Hyperoxia-induced methylation decreases RUNX3 in a newborn rat model of bronchopulmonary dysplasia. Respir Res 2015;16:75.
12. Jagarapu J, Kelchtermans J, Rong M, Chen S, Hehre D, Hummler S, et al. Efficacy of leukadherin-1 in the prevention of hyperoxia-induced lung injury in neonatal rats. Am J Respir Cell Mol Biol 2015;53:793-801.
13. Han T, Chi M, Wang Y, Mei Y, Li Q, Yu M, et al. Therapeutic effects of fibroblast growth factor-10 on hyperoxia-induced bronchopulmonary dysplasia in neonatal mice. Am J Transl Res 2017;9:3528-40.
14. Das KC, Ravi D. Altered expression of cyclins and cdks in premature infant baboon model of bronchopulmonary dysplasia. Antioxid Redox Signal 2004;6:117-27.
15. Johansson A, Hampel H, Faltraco F, Buerger K, Minthon L, Bogdanovic N, et al. Increased frequency of a new polymorphism in the cell division cycle 2 (cdc2) gene in patients with Alzheimer's disease and frontotemporal dementia. Neurosci Lett 2003;340:69-73.
16. Nigg EA, Blangy A, Lane HA. Dynamic changes in nuclear architecture during mitosis: on the role of protein phosphorylation in spindle assembly and chromosome segregation. Exp Cell Res 1996;229:174-80.
17. Singhal S, Amin KM, Kruklitis R, DeLong P, Friscia ME, Litzky LA, et al. Alterations in cell cycle genes in early stage lung adenocarcinoma identified by expression profiling. Cancer Biol Ther 2003;2:291-8.
18. Choi JM, Shin JH, Sohn MH, Harding MJ, Park JH, Tobiasova Z, et al. Cell-permeable Foxp3 protein alleviates autoimmune disease associated with inflammatory bowel disease and allergic airway inflammation. Proc Natl Acad Sci U S A 2010;107:18575-80.
19. Zhao H, Yang B, Xu J, Chen DM, Xiao CL. PM2.5-induced alterations of cell cycle associated gene expression in lung cancer cells and rat lung tissues. Environ Toxicol Pharmacol 2017;52:77-82.
20. Adams MN, Burgess JT, He Y, Gately K, Snell C, Zhang SD, et al. Expression of CDCA3 Is a prognostic biomarker and potential therapeutic target in non-small cell lung cancer. J Thorac Oncol 2017;12:1071-84.
21. Lewis DL, Wolff JA. Delivery of siRNA and siRNA expression constructs to adult mammals by hydrodynamic intravascular injection. Methods Enzymol 2005;392:336-50.
22. Guo Z, Li Q, Han Y, Liang Y, Xu Z, Ren T. Prevention of LPS-induced acute lung injury in mice by progranulin. Mediators Inflamm 2012;2012:540794.
23. Nicola T, Ambalavanan N, Zhang W, James ML, Rehan V, Halloran B, et al. Hypoxia-induced inhibition of lung development is attenuated by the peroxisome proliferator-activated receptor-γ agonist rosiglitazone. Am J Physiol Lung Cell Mol Physiol 2011;301:L125-34.
24. Jobe AH. Mechanisms of lung injury and bronchopulmonary dysplasia. Am J Perinatol 2016;33:1076-8.

25. Wang L, Lu H, Li M. Expression of angiopoietin-1 and lung development in neonatal rat with hyperoxia-induced BPD. J Clin Pediatrics 2014;(4):355-9.
26. Megonigal MD, Rappaport EF, Jones DH, Williams TM, Lovett BD, Kelly KM, et al. t(11;22)(q23;q11.2) in acute myeloid leukemia of infant twins fuses MLL with hCDCrel, a cell division cycle gene in the genomic region of deletion in DiGeorge and velocardiofacial syndromes. Proc Natl Acad Sci U S A 1998;95:6413-8.
27. Tang WJ, Peng KY, Tang ZF, Wang YH, Xue AJ, Huang Y. MicroRNA-15a - cell division cycle 42 signaling pathway in pathogenesis of pediatric inflammatory bowel disease. World J Gastroenterol 2018;24:5234-45.
28. Siow JK, Alshaikh NA, Balakrishnan A, Chan KO, Chao SS, Goh LG, et al. Ministry of health clinical practice guidelines: management of rhinosinusitis and allergic rhinitis. Singapore Med J 2010; 51:190-7.
29. Cai C, Qiu J, Qiu G, Chen Y, Song Z, Li J, et al. Long non-coding RNA MALAT1 protects preterm infants with bronchopulmonary dysplasia by inhibiting cell apoptosis. BMC Pulm Med 2017;17: 199.
30. Ogunlesi F, Cho C, McGrath-Morrow SA. The effect of glutamine on A549 cells exposed to moderate hyperoxia. Biochim Biophys Acta 2004;1688:112-20.
31. Hansel DE, Dhara S, Huang RC, Ashfaq R, Deasel M, Shimada Y, et al. CDC2/CDK1 expression in esophageal adenocarcinoma and precursor lesions serves as a diagnostic and cancer progression marker and potential novel drug target. Am J Surg Pathol 2005; 29:390-9.
32. Blick C, Ramachandran A, McCormick R, Wigfield S, Cranston D, Catto J, et al. Identification of a hypoxia-regulated miRNA signature in bladder cancer and a role for miR-145 in hypoxia-dependent apoptosis. Br J Cancer 2015;113:634-44.
33. Zhang S, Guo Y, Zhang C, Gao W, Wen S, Huangfu H, et al. Primary laryngeal cancer-derived miR-193b induces interleukin-10-expression monocytes. Cancer Invest 2015;33:29-33.
34. Rancourt RC, Keng PC, Helt CE, O'Reilly MA. The role of p21(CIP1/WAF1) in growth of epithelial cells exposed to hyperoxia. Am J Physiol Lung Cell Mol Physiol 2001;280:L617-26.
35. McAdams RM, Vanderhoeven J, Beyer RP, Bammler TK, Farin FM, Liggitt HD, et al. Choriodecidual infection downregulates angiogenesis and morphogenesis pathways in fetal lungs from Macaca nemestrina. PLoS One 2012;7:e46863.
36. Pan J, Zhan C, Yuan T, Wang W, Shen Y, Sun Y, et al. Effects and molecular mechanisms of intrauterine infection/inflammation on lung development. Respir Res 2018;19:93.
37. Wu L, Qin Y, Xia S, Dai M, Han X, Wu Y, et al. Identification of cyclin-dependent Kinase 1 as a novel regulator of type I interferon signaling in systemic lupus erythematosus. Arthritis Rheumatol 2016;68:1222-32.
38. Du J, Wei N, Guan T, Xu H, An J, Pritchard KA Jr, et al. Inhibition of CDKS by roscovitine suppressed LPS-induced *NO production through inhibiting NFkappaB activation and BH4 biosynthesis in macrophages. Am J Physiol Cell Physiol 2009;297:C742-9.

https://doi.org/10.3349/ymj.2020.61.8.679